

Spatial Self-Reorganization of Repulsive Mobile Agents

Jacques Henri Collet, and Jean Fanchon

CNRS; LAAS; 7 avenue du colonel Roche, F-31077 Toulouse, France
Université de Toulouse; UPS, INSA, INP, ISAE; LAAS; F-31077 Toulouse, France
7 avenue du colonel Roche, 31077 Toulouse Cedex 07
jacques.collet@laas.fr, jean.fanchon@laas.fr

Abstract

We study the self-reorganization of large sets of agents moving in finite 2-dimensional spaces, under the effect of local repulsion laws. Agents are partitioned in two subsets (populations) and tend to move away from their neighbors lying in a local sense disk, following a force-inspired law. The contribution of a neighbor to the movement of an agent depends on whether they belong to the same population or not. First, we show that the ratio of the intensity between intra-population and inter-population repulsions is a critical parameter leading either to macroscopic separation, where agents are separated in different homogeneous regions depending on their state, or simply to local reorganization. We then show that the reorganizations are effective only above a sharp threshold of the collision rate between agents. We also present an application to swarm robotics, where a fleet of carrying robots self-organizes in collision-free streams of robots moving in the same direction, under the effect of the repulsion algorithm.

Key words

Self-reorganization, separation, repulsion, transportation

1 Introduction

Massive mobile multiagent systems have been widely investigated in recent years in many fields like swarm robotics [1], sensor networks [2], sociology [3,4,5,6,7], animal life [8], games, etc.. Two outcomes of such mobile multiagent systems may be distinguished:

- The spatial aspect: what are the resulting spatial configurations, the resulting movements, which relations exist between these locations and/or movements?
- The data computational aspect: which data are being manipulated, and exchanged, which operations are executed on these data, and what are the resulting values?

We are primarily concerned with the first of these aspects. Our goal is to contribute to defining simple agent algorithms which could be considered as primitive building blocks to induce some macroscopic and controlled spatial properties, like specific distributions or movements of the agents. These primitives are meant to be used as behavioral components in larger applications [9,10]. Here, the algorithms are simple and consume little memory or computing power.

The agents that we consider move in a finite 2-dimension space and their knowledge of the environment is local, restricted to a sense or communication neighborhood around them. We consider two populations of agents (implemented as agent states). At each step of his behavior, an agent computes a move direction, which depends on the neighbors in his sense disk.. Each agent follows a force-inspired rule to decide a move [11,12,13,14,15,16,17], the direction of which results from two components: a repulsion computed from the neighbors in the same population (intra population repulsion, denoted IntraPopR) and the repulsion computed from agents in another population (inter-population repulsion, denoted InterPopR). The relative contribution of a neighbor to the repulsion law depends on his distance to the agent. This implies in particular that the agents are able, either by communication or direct sensing, to determine the relative positions and local states (type of population) of their neighbors. Consequently, it is important to underline that the system evolves exclusively due to repulsion mechanisms between sets of agents confined in a finite area.

In what follows, we first study the conditions of spontaneous separation of the populations following an initial state where the agents are created randomly in position, direction and state. We show that the dynamics and the properties of the separation critically depend on the ratio of InterPopR to IntraPopR forces. We observe 3 typical behaviors at high density of agents (i.e., when the average number of agents found in the sense disk exceeds typically 1, see full definition in the beginning of section 3):

- When InterPopR is stronger than IntraPopR, self-reorganization of populations makes that agents are separated in different homogeneous regions depending on their state. We observed this coarse-grained separation as soon as InterPopR is 1% larger than IntraPopR. The more repulsion laws (between populations) are unbalanced, the more the separation is a fast process accompanied by the emergence of a regular empty space between adjacent regions. This empty space disappears when repulsions become balanced.
- When InterPopR and IntraPopR repulsions are identical, the two populations evolve but stay in a random topological state.
- When InterPopR are weaker than IntraPopR, there is a local order instead of a coarse-grained separation.

We made separation study quantitative by studying the evolution of the average number of agents of each population in sense disk, and by analyzing the influence of the agent density on the separation mechanism.

These simple repulsion laws and the resulting properties offer various perspectives in multiagent systems. In the last section of the paper, we present an application to swarm robotics, for a fleet of carrying robots. Robots move back and forth between a loading and a dropping zone, and under the sole effect of the repulsion algorithm, self-organise in streams where all agents move in the same direction, creating unidirectional collision-free separated corridors.

The manuscript is organized in 6 parts as follows: In section 2, we describe how the agent calculates his move. We describe in section 3 the simulations which display the separation of the two populations. In section 4, we study the conditions of separation by calculating (from simulations) the temporal evolution of the average numbers of each type of agents in the sense disk. The efficiency of the separation versus the agent density is studied in section 5. In section 6, we show the application of the simple local rules to the problem of transportation and the formation of unidirectional corridors.

2 Agent description and properties

Each agent is identified by three parameters, namely: 1) His index i , i.e., in the set of agents; 2) His internal state s_i , conventionally 0 or 1. Population 0 is the population of agents in state 0, and population 1 that of agents in state 1; 3) His spatial location defined by the vector \vec{P}_i of components (x_i, y_i) . Each agent also knows the positions and status (population) of the surrounding agents inside a sense disk of radius d . The way the agent knows the position and status of the other agents inside this disk is not the subject of this paper. However, it could be achieved by direct sensing, sense or inter-agent communications.

2.1 Move direction

In what follows, we extend the definition of the move direction that we introduced in [14] to describe the evolution of one sole population of repulsive agents. The move direction $\vec{D}(i)$ of the agent of index i is the sum of two terms, namely:

$$\text{Eq. 1} \quad \vec{D}(i) = K_1 \vec{D}_1(i) + K_2 \vec{D}_2(i)$$

$\vec{D}_1(i)$ is the direction vector due to the interaction with the agents in the same state inside the sense disk We shall say conventionally that the vector $\vec{D}_1(i)$ comes from intra-population interactions. Vector

$\vec{D}_2(i)$ comes from the interaction with the agents in the other state and we shall say that it results from inter-population interactions. K_1 and K_2 are two coefficients to adjust the relative contribution of $\vec{D}_1(i)$ and $\vec{D}_2(i)$. Each direction vector depends on the distribution of agents inside the sense disk. We chose the following law for interactions between agents in the same states:

$$\text{Eq. 2} \quad \vec{D}_1(i) = \sum_{\substack{\text{agents } j \text{ in the same state} \\ \text{inside sense disk } \text{Disk}(r_i, R)}} |\vec{p}_i - \vec{p}_j|^{-n_1} \vec{u}_{ij}$$

where:

- $|\vec{p}_i - \vec{p}_j| = \sqrt{(x_i - x_j)^2 + (y_i - y_j)^2}$ is the Euclidian distance between the agents of indexes i and j , and $\vec{u}_{ij} = (\vec{p}_j - \vec{p}_i) / |\vec{p}_i - \vec{p}_j|$ the unitary direction vector from point i to point j .
- n_1 is a real coefficient. We are fully free to setup the values of the coefficients n_1 and n_2 depending on the agent behavior we target. For instance, $n_1=2$ and $K_1<0$ makes that the agents will partly mimic the electrostatic interactions between charged particles because the agent-agent "force" decays as the square of the distance.

The equation defining the vector $\vec{D}_2(i)$ is similar to Eq. 1, except that n_2 replaces n_1 and that the sum runs over the agents in the other state. The move direction move defined by Eq. 1 and Eq. 2 depends on five scalar parameters, namely K_1 , K_2 , n_1 , n_2 , and the sense radius R . Note the importance of the sign. $K_1<0$ makes that an agent will move away from the agents in the same population, and we implement intra-population repulsion (IntraPopR). Contrarily, $K_1>0$ implements intra-population attraction. Similarly, depending on the sign of K_2 , we may implement repulsion or attraction between the agents in different populations. We must also underline that, at first sight, it might seem that the two coefficients K_1 , K_2 , define four degrees of freedom, namely, the sign and the modulus of K_1 and K_2 , respectively. However, the move direction in Eq. 1 stays unchanged when $|K_1|/|K_2|$ is constant. For instance, the move direction is unchanged (other things being equal) when ($K_1=2$, $K_2=-3.2$) or ($K_1=4$, $K_2=-6.4$). Consequently, because we only consider repulsive agents in the following, we shall set $K_1=-1$ without reducing the generality of our analysis.

2.2 Agent state automaton and move decision

We now describe the state automaton executed by each agent and the resulting move. Possible moves are restricted to the eight cells directly adjacent to the agent position in a 2D mesh topology. The agent makes a move decision following the next algorithm:

1. When he detects no agent inside his sense disk, he continues to move in pursuing its current direction. In section 5, we shall also consider the case when the agent stops instead of moving. State 1 plays no significant part in the agent evolution at high density (section 3)
2. When he detects agents inside his sense disk, he moves following the direction defined in the preceding section 2.1.
3. There is a collision between two agents when the final cell (calculated by the two above rules) is already occupied. To define a move even in this case, the agent first identifies the eight cells adjacent to his position by their directions $\vec{C}_n = (\cos(n\pi/4), \sin(n\pi/4))$ with $0 \leq i < 8$. Then, he scans these cells in the ascending order of the angle (\vec{C}_n, \vec{D}_i) with the "ideal direction" and chooses the first free cell. The agent does not move if no adjacent cell is free.

2.3 Brief simulator description

The simulations reported in the next sections were conducted with the simulator MASS (Mobile-Agent Set Simulator). MASS is an application, the full description of which is beyond the scope of this publication.

However, an extended documentation⁽¹⁾ and even the simulator can be downloaded from the web page <http://www.laas.fr/~collet>. The simulator works in the Windows environment and exhibits a highly interactive interface necessary to trace the collective effects appearing in the "large" populations. MASS calculates the collective behavior of thousands agents from the evolution of each agent, which follows the rules of its state automaton. Usually, it works smoothly and interactively for populations comprising up to a few tens of thousands of agents, depending on the complexity of the agent state automaton. The activation of agents is based on the following paradigm:

- Each agent has an internal time parameter, which is his next activation time (NAT). A scheduler scans all agent NATs and activates the agent with the shortest NAT.
- The activated agent scans its environment to identify the other agents inside a sense disk. Then, it chooses a move following the rules described in section 2.2.
- Finally, the activated agent increments his NAT and returns the control to the scheduler, which scans again all agent NATs to activate the agent with the shortest NAT, and so on. As all agents have the same time increment when they increment their NAT, all agents are sequentially activated in these simulations. When an agent is activated, it is aware of the moves previously executed by the other agents.

3 Separation in high-density populations

The high density regime is reached when the average number of neighbors \bar{n}_{SD} that an agent identifies inside his sense disk is larger than 1. Concretely, this means that, in this regime, each agent is almost always colliding with one or several agents and consequently, he is almost never in the state 1 of his automaton (see section 2.2). The mathematical condition which characterizes the high-density regime is simply:

$\bar{n}_{SD} = n\pi R^2 / S > 1$, where R is the sense radius, S the terrain area, and n the total number of agents. Our simulations were conducted with the conditions: $N_x=400$, $N_y=300$ (rectangular terrain dimension counted in cells), $n_1=n_2=500$ (agent number), $R=40$ (sense disk radius) so that we deduce $\pi(n_1 + n_2)R^2 / N_x / N_y \approx 45$. Moreover, we applied cyclic boundary conditions (CBC). CBC is a useful trick to limit the influence of the borders on the evolution of the populations. Simply, when an agent hits a border, he disappears and reappears on the opposite border with the same move direction. Of course, the separation effects reported in the rest of this work persists in the presence of borders, but CBC make behaviors ultimately simpler.

Note that the respective influence of IntraPopR and InterPoPR depends on the relative amplitude of the two vectors $\vec{D}_1(i)$ and $\vec{D}_2(i)$ in Eq. 1. It is therefore perfectly possible to change the contributions of intra and inter repulsions by changing the indexes n_1 and (or) n_2 . However, in this study, we only analyze the "Coulomb-like" case corresponding to $n_1=n_2=2$ (see Eq. 2), and we study the spatial evolutions of the agent populations depending on the value of the inter-population coupling $K_2 \leq 0$ assuming $K_1=-1$ (following discussion in section 2.1). The system starts from a population randomly generated both in space, state and initial direction. There is approximately the same initial number of agents in states 0 and 1.

Before we describe in details the simulation results, we must underline the fluctuation problem that we encountered. This problem is that, starting from two different initial distributions obtained by random generation of agents, we observe different but similar coarse-granularity evolutions which in the long term preserve the quasi-stationary macroscopic and spatial properties of the system. In other words, separation is a universal effect, but the transient regime strongly fluctuates to lead to stable high-symmetry populations that we study in the next sections.

⁽¹⁾ This site includes three manuals (at all, more than 400 pages of documentation) to explain how using MASS (Tutorial.pdf), how customizing MASS (DLLs Manual.pdf), and how MASS works (CORE Manual.pdf). The web site also includes several animated images, which display the transient dynamics of the agent population corresponding to the studies discussed in this work. MASS at the moment represents approximately five man×years of C++ programming, and it is under permanent development.

3.1 Strong inter-population repulsion ($-16 < K_2 < -2.5$)

This case occurs when InterPopR are much stronger than IntraPopR, i.e., when $K_2 < 0$ and $|K_2 / K_1| \gg 1$. Typical distributions are shown in Fig. 1. Fig. *a* is an example of initial random distribution. Figs. *b,c,d* show typical stationary states that can be observed when each agent is activated 1000 times. We always observe the separation of agents which group together in homogeneous zones (i.e., composed of agents in the same state), which grow in size, and aggregate. We must stress that the final topology is unpredictable, except that the system always evolves toward a high symmetry topological state.

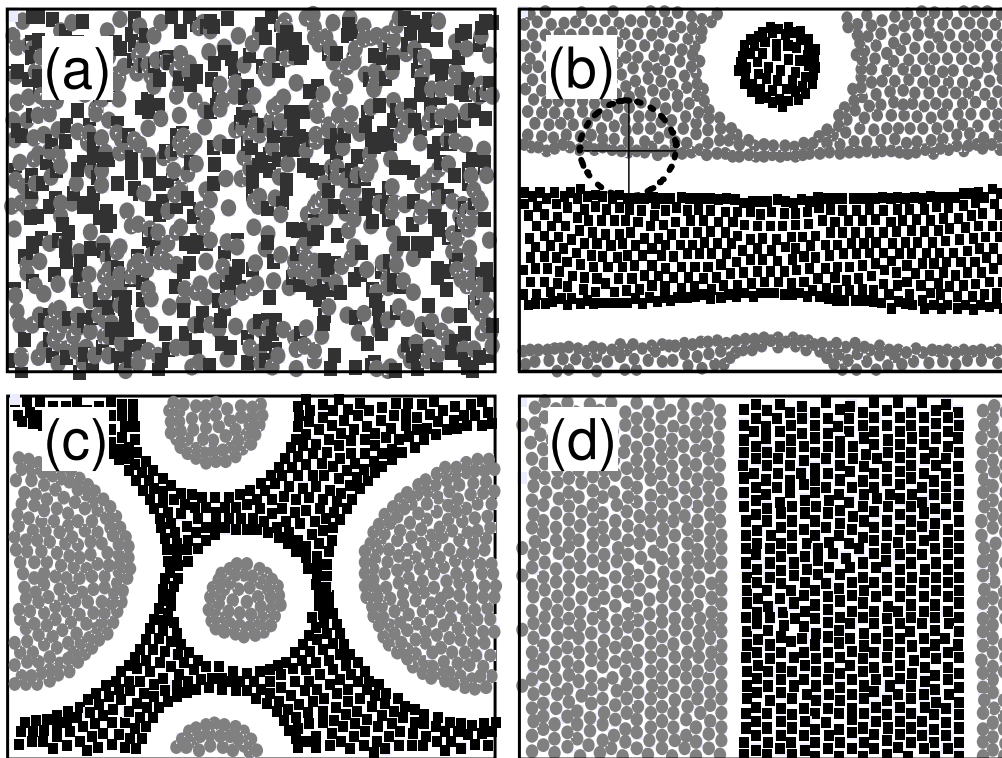


Fig. 1: Evolution of populations when interPopR is strong. Black squares are agents in state $s=0$, and grayed circles represent agents in state $s=1$. Common simulation parameters: $LX=400$, $LY=300$, $N=1000$, $R=40$, $n_1=n_2=2$, cyclic boundary conditions in X and Y directions. Fig b: $K_2=-16$; Fig c: $K_2=-8$; Fig d: $K_2=-2.5$. (a): Typical initial random distribution;

Fig *b* shows an example of separation of the two populations when $K_2=-16$, Fig *c* show an evolution when $K_2=-8$, and finally Fig *d* shows an evolution when $K_2=-2.5$. This last figure is especially striking as it shows that full separation into two non-interlaced "phase" is possible. We must underline that the full separation reported in Fig *d* when $K_2=-2.5$ occurs as well in the simulations reported in Figs *b* and *c* with the same degree of unpredictability. Moreover, Fig. 1 reveals two puzzling effects:

1. We can observe a kind of no-man's-land (NML) between the different zones, the width of which depends on K_2 . When the inter-population repulsion is very strong (see Fig. *b*, when $K_2/K_1=16$), the width of the NML equals practically the radius of the sense disk, and diminishes when $|K_2|$ diminishes. This result is no real surprise. It simply means that the inter-population repulsion is so strong that an agent, who enters the sense disk of an agent of the other population, feels immediately strong repulsion which pushes him back outside the sense disk.
2. There is a kind of skin effect when the intensity of InterPopR is much stronger than that of IntraPopR. The skin effect makes that the density of agents increases very close to the interface of a cluster or any simple connected homogeneous zone (see Fig. 1*b* and *c*), just at the border of the no-man's-land.

3.2 Slightly unbalanced repulsion ($-1.15 \leq K_2 < -1$)

We define repulsions as being "slightly unbalanced" when the intensity of interPopR is slightly stronger than that of the intraPopR, say typically when $-1.15 \leq K_2/K_1 < -1$. The figures below show that the separation takes place in the long term when inter- and intra- population repulsions are unbalanced, even if the difference is very small. Fig. b is especially interesting as it shows clear separation in the long term when inter-population repulsion exceeds intra-population repulsion by only 1%. However, it must be stressed that the separation mechanism becomes extremely slow as Fig. b was recorded following 5×10^5 execution cycles whereas the distributions in Fig. 1 were recorded following only a few thousands of cycles. Nevertheless, it is demonstrated that the separation results from small moves of each agent to one of its 8 adjacent cells, without assuming long-distance move (as in [] to satisfy a criteria of minimum global repulsion).

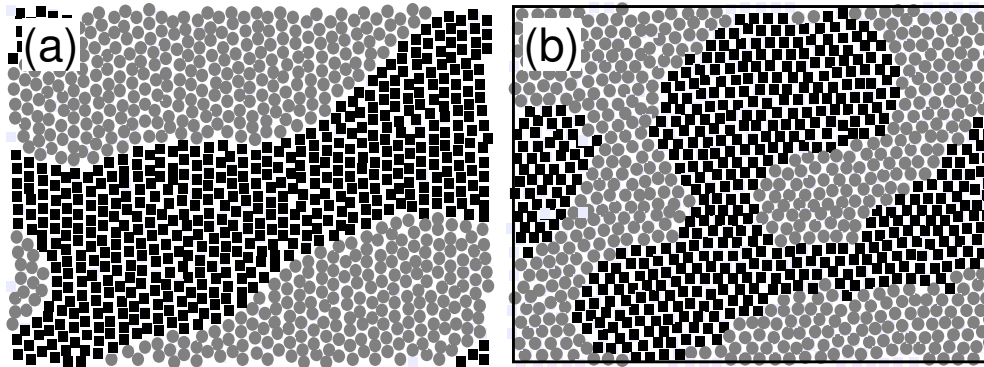


Fig. 2: Evolution of populations when intra- and inter-population repulsions are slightly unbalanced. Black squares are agents in state $s=0$, and grayed circles represent agents in state $s=1$. Common simulation parameters are exactly those of Fig. 1. Fig a: $K_2=-1.15$ (following 4500×12 iterations); Fig b: $K_2=-1.01$ (following $4500 \times 24 \times 2.5$ iterations).

3.3 Weak inter-population repulsion ($-1 < K_2 < 0$)

In this regime, InterPopR become weaker than IntraPopR while we studied the opposite case from the beginning of section 3. Two typical long-term distributions are shown in Fig. 3.

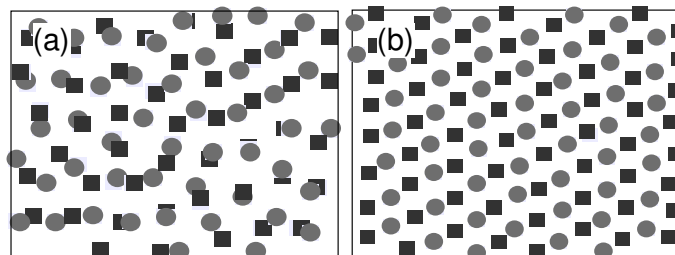


Fig. 3: Evolution of the agent distribution when inter-population repulsions is small. Black squares are agents in state $s=0$, and grayed circles represent agents in state $s=1$. Common simulation parameters are exactly those of Fig. 1. Fig a: $K_2=0$; Fig b: $K_2=-0.5$.

Note that the two figures display only 1/9 of the full terrain to highlight the local changes. It is clear that there is no coarse agent separation as observed in Fig. 1 and Fig. 2 but contrarily, local changes around each agent. We observed three typical evolutions:

- When $K_2=K_1=-1$, IntraPopR and InterPopR are identical. Therefore, the displacement calculated by an agent no longer depends on the type of agents detected in the sense disk, and everything happens as if there was only one population of agent! Thus, we recover the single-population case that we extensively studied in [14]. We observe the expansion of the agent distribution, which consists in occupying uniformly the space. Of course, there always persist local fluctuations of the agent density, but the average density is uniform in the long term.

- The situation is very similar to the previous one when $K_2=0$ because we consider two populations of agents, which ignore each other almost perfectly. The sole coupling which persists comes from the fact that two agents cannot occupy the same cell (see the agent automaton in section 2.2). This coupling is very weak. Therefore, this case comes to studying two independent populations at half density, and we observe interlaced distributions which occupy randomly the terrain. A typical long-term distribution achieved in this case is displayed in Fig. 3a.
- When $-1 < K_2 < 0$, we always observe a local organization, or in other words, a short-range order, because each agent tends to be mostly surrounded by agents of the other population. This effect is clearly evidenced in Fig. 3b. The system has evolved here toward the alternation of vertical lines made up with one sole population of agents. However, we also observed some other local reorganizations, for instance toward two interlaced squared lattices, each one being build up with one single population. Also, the mixture of the above distributions is possible. The evolution over the long term toward a particular local reorganization is an unpredictable phenomenon. Moreover, the appearance of the local order becomes very slow when K_2 is close to 0 or -1, which is no surprise since it is close to the limit case without local order that we described just above.

4 Kinetics of separation

Section 3 presented a necessary classification of population evolutions. The description was qualitative, but it shows that separation of population takes place when $|K_2/K_1| > 1.01$ and that no macroscopic effect (with a spatial extension of the order of the radius) occurs when $-1 < K_2 < 0$. To study more quantitatively the separation, we calculated for each agent the number $n_S(i)$ of agents in the same state inside its sense disk, then the number $n_D(i)$ of agents in the different state. i is the agent index. Then, we used as separation metrics the average values $\bar{n}_S = \sum_i n_S(i)$ and $\bar{n}_D = \sum_i n_D(i)$. The temporal evolution of these two averages is displayed in Fig. 4. The lines below the horizontal line $n=19$ show the evolution of \bar{n}_D , i.e., the diminution of the number of agents of the other population inside the sense disk (due to the spatial separation of agents) and the upper lines shows the increase of \bar{n}_S for the agents of the same population.

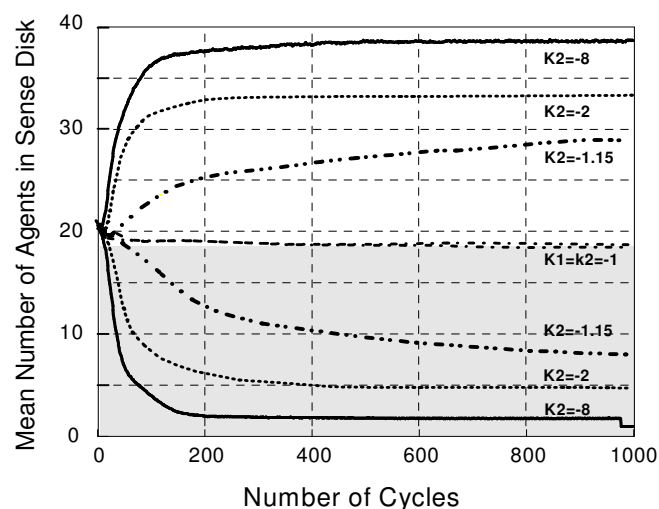


Fig. 4: Evolution of the average number of agents in the sense disk. Upper curves display the increase of the number of agents in the same population and lower curves (in the grayed rectangle) the decrease of agents of the other population. Simulation parameters are exactly those of Fig. 1. When $K_1=K_2=-1$, the average numbers for each population is stable around 19 and there no evidence of separation.

Each simulation is therefore characterized by 2 curves. Fig. 4 shows that they are quasi-symmetric with respect to the horizontal line $N=19$! It simply means that agents which move away are replaced

by agents of the same population and that the average density $\bar{n}_D + \bar{n}_S$ (considering the two populations) stays quasi-constant during evolution that can be observed in Fig. 2 and Fig. 3. The sole notable exception occurs in the no-man land displayed in Fig. 1.

5 Influence of the agent radius on separation

It is totally obvious that the macroscopic-separation phenomenon comes from the agent repulsions resulting from agent-agent collisions. There are two solutions to change the frequency of collisions, i.e., the number of neighbors that an agent sees inside his sense disk. One may shrink the agent radius or diminish the number of agents in the terrain. In this section we chose the first method, other things being equal. The simulation conditions as those of Fig. 1, i.e., terrain size: $S=400 \times 300$, number of agents: $n=1000$, $K_2/K_1=8$, $n_1=n_2=2$, agents are initially equally and randomly distributed in two states. The figures (a) and (b) below display the average number of agents seen in the sense disk when the agent radius varies from 6 to 50. This is the long-term average number of agents, following the inevitable transient regime of spatial reorganization already analyzed in Fig. 4.

In Fig. 5 a, the agent stays immobile when he detects no neighbor inside his sense disk. The fact that the agents do not move (Fig. a) induces an abrupt mobility threshold when the radius is smaller than the average inter-agent distance. The reason is simply that, in this case, there are enough places for all agents in the terrain without overlap of their sense disks. Therefore, each agent stops moving following some initial transient phase of mutual repulsions! It is easy to estimate the radius associated to this mobility threshold. Let us assume that the agents are approximately located on the vertices of a 2D mesh. The average agent-agent distance d would be approximately $d = \sqrt{S/N} \approx 11$ in our study. The distance d would be even slightly larger if agents were located on the vertices of a hexagonal lattice. Note that it is exactly what Fig. 5a shows! The square points represent the average number of agents (ANA) of each type seen in the sense disk when $K_1=K_2$. Because Intra- and Inter- population repulsions are identical, there is no separation and the average number of agents seen in the sense disk is the same for each population. It can be seen that when the radius R changes from 10 to 12, the number of agents increases of about 2 orders of magnitudes to reach about 1. This threshold persists when repulsions are asymmetric with $K_2/K_1=8$. The upper dotted line in Fig. 5a shows the variations of the number of agents of the same population seen in the sense disk, whereas the bottom triangle line shows the number of agents of the other population.

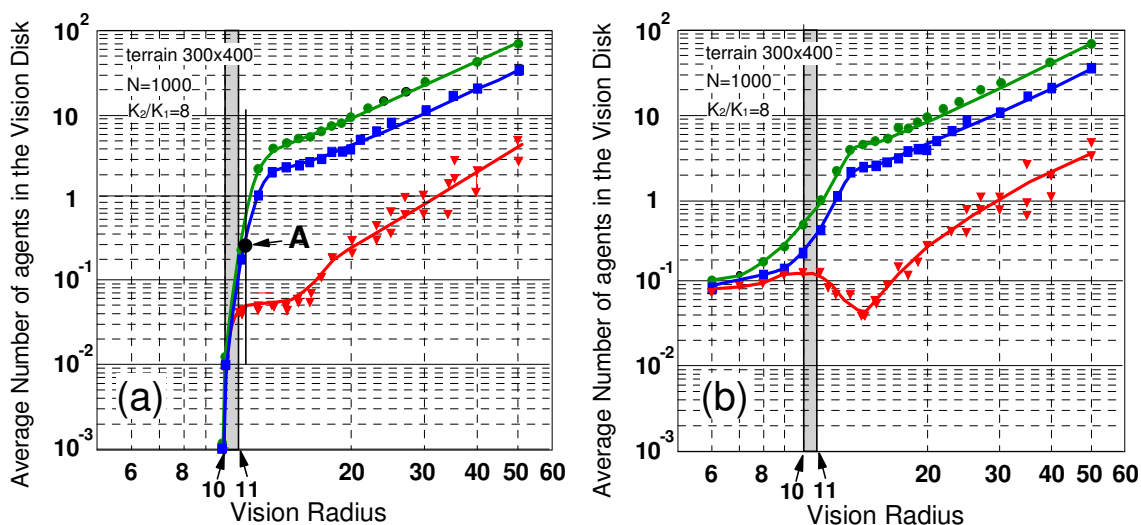


Fig. 5: Steady state number of agents in the sense disk. Common parameters: $N=1000$, terrain: 400×300 . Square points: $K_2=K_1$, half of the number of agents in the sense disk; Circles: $K_2/K_1=8$, number of agents of the same population; triangles: $K_2/K_1=8$, number of agents of the other population. Left

figure (a): The agent does not move when it sees no agent inside his sense disk; Right figure (b): The agent keeps moving in his current direction when he discovers no agent in his sense disk.

Let us define the separation parameter S as the average number of agents in the sense disk belonging to same population N_I divided by the number of agents belonging to the other populations N_D . Perhaps, the most striking result evidenced in Fig. 5a is that the long term separation immediately reaches $S=20-30$ above the radius threshold (i.e., when $R>12$) and remain stable up to $R=50$. There is no smooth progression of the separation mechanism. This is a very effective process as soon as collisions occur. Indeed, point A in Fig. 5a shows that even if ANA is about 0.3 (in other words, if there is one collision every third agent activation), the separation is very high, as S is around 20-30.

Fig. 5b duplicates the separation study shown in Fig. 5a, except that an agent continues to move in his current direction when he detects no agent inside his sense disk. Consequently, there is no mobility threshold and the agents do not stop moving at low density or equivalently when the sense radius is small. Note that Fig. 5a and b show the same separation of the populations at high density (i.e., when the average number of agents seen in the sense disk exceeds typically 4-5) because all agents almost always detect other agents and therefore follow the same behavioral rules. Below the radius threshold (around $R=12$), collisions are weak but persists in Fig. 5b without triggering a significant separation of populations.

6 Direct application: Self-organizing streams of agents

We briefly present now an example showing the practical interest of the repulsion principle, which enlarges the perspectives of its use in concrete problems. We consider here populations which are characterized by an intended direction in the 2D space: agents are carrying robots divided in two classes, *empty* robots which move towards a loading zone and pickup an object, *loaded* ones which move towards a dropping zone and drop their load. After dropping or picking, agents change their state and their intended direction, accordingly. Furthermore their move direction is computed as specified in Eq. 3 below, with an additional component $K_3 \vec{D}_3(i)$, where $\vec{D}_3(i)$ is the unit vector indicating the intended direction and K_3 the weight of the new component .

Eq. 3
$$\vec{D}(i) = K_1 \vec{D}_1(i) + K_2 \vec{D}_2(i) + K_3 \vec{D}_3(i)$$

Fig 6a shows a remarkable resulting global property, which appears for appropriate values of the parameters in Eq 3: the creation of unidirectional collision-free corridors. The agents in these corridors behave like the members of self-organized flocks [18] induced by a very simple algorithm.

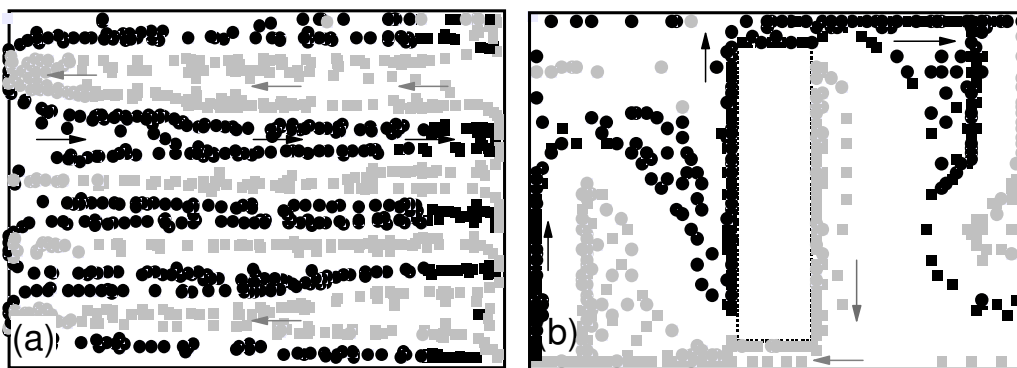


Fig. 6: Agents circulation without (a) and with obstacles (b). In both figures, the agent streams follow the arrows between the left and right borders. The sense radius is 20 in both simulations; Parameters in fig. (a): $n_1 = 1, n_2 = 1, K_1 = -1, K_2 = -4, K_3 = 2$, terrain = 400x300, agent number = 1000. Parameters in fig. (b): $n_1 = 1, n_2 = 0.5, K_1 = -1, K_2 = -3, K_3 = 2$, terrain = 100x70, agent number = 500.

In this example, the separation property still heavily relies on a low ratio between InterPopR and IntraPopR, but also on their strength relative to the new component. The case of figure 6a is achieved by setting the val-

ues of parameters as follows: $n_1 = n_2 = 1$, $K_1 = -1$, $K_2 = -4$ and $K_3 = 2$. Let us note that the value -1 of the exponents n_1 and n_2 is different from the value -2 used in the previous sections. It increases the strength of the repulsion components, and decreases the impact of the distance between the agents.

Another noteworthy consequence of repulsions appears when a large obstacle separates the loading and dropping zones as depicted in Fig 6b. It shows that, for particular values of the parameters, the agent streams may establish a stable collision-free round-trip circulation between the two zones around the obstacle, following the direction highlighted by the arrows along the lines of [19,20].

7 Conclusion and perspectives

This work demonstrates that in confined environment, the simple use of repulsion laws induces interesting and usable effects. We observed spontaneous separation and showed that the ratio of the intensity between intraPopR and interpopR is a critical parameter, which governs the mechanism. We also showed that the repulsion laws can be successfully applied to more concrete problems such as self-organized transportation. A promising field of investigation lies in the dynamic modification by an agent of the weights of its different direction components, or of its sense radius, depending on its local context. This should lead to self-adaptive algorithms able to deal with congestions, scarce density, etc..

References

- [1] Y. U. Cao, A. S. Fukunaga, and A. B. Kahng, "Cooperative mobile robotics: Antecedents and directions," *Autonomous Robots*, vol. 4, pp. 7-27, (1997)
- [2] M. Tubaishat and S. Madria, "Sensor networks: An overview," *IEEE Potentials*, vol. 22(2), pp. 20-23, (2003).
- [3] Thomas Schelling, "Dynamic model of segregation", *Journal of Mathematical Sociology*, vol 1, pp 143-186, (1971)
- [4] M. Fossett, "Ethnic preferences, Social Distance Dynamics, and Residential segregation: Theoretical explorations using simulation analysis", *The Journal of Mathematical Sociology*, vol 30(3), pp 185-273,(2006)
- [5] J. Zhang, "A dynamic model of residential segregation", *Journal of Mathematical Sociology*, vol 28, pp 147-170, (2004)
- [6] W.A.V. Clark, and M. Fosset, "Understanding the social context of the Schelling segregation model", *PNAS*, vol 105(11), pp 4109-4114, (2008)
- [7] A. Singh, D. Vainchtein, H. Weiss, "Schelling's segregation model: parameter, scaling, and aggregation", *Demographic Research*, vol 21, pp 341-366, (2009)
- [8] K.A. Hawick, C.J. Scogings, and H.A. James, "Defensive spiral emergence in a predator-prey model"; *Proc. 7th Asia-Pacific Conference on Complex systems*, (2004), ISSN 1320-0682
- [9] D.Coore. "Abstractions for Directing Self-organising Patterns" *UPP 2004, LNCS 3566*, pp. 110-120, (2005)
- [10] I. Suzuki, and M. Yamashita: "Distributed anonymous mobile robots: Formation of geometric patterns." *SIAM Journal of Computing* 28(4), 1347-1363 (1999)
- [11] K. Hussain, E. Gelenhe, and V. Kaptal, "Simulating the Navigation and Control of Autonomous Agents", *Proc. Fusion 2004: Seventh International Conference on Information Fusion; Stockholm; Sweden; 28 June-1 July 2004.* (2004)
- [12] F. Getcher, V. Chevrier, and F. Charpillet, "A reactive agent-based problem-solving", model: Application to localization and tracking, *ACM Transactions on Autonomous and Adaptive Systems (TAAS)*, vol 1(2), pp 190-222, (2006)
- [13] M. Scheutz, and M. Bauer, , "A scalable, robust, ultra-low complexity agent swarm for area coverage and interception tasks, *2006 IEEE International Conference on Control Applications, Symposium on Intelligent Control*, pp.1258-1263, (2006)
- [14] J.H. Collet, "Order-Disorder Alternations in the Populations of Faulty Repulsive Agents", *Physica A*, vol 386, pp 345-364, (2007)
- [15] S. Yang, F. Gechter, A. Koukam , "Application of Reactive Multi-agent System to Vehicle Collision Avoidance", *20th IEEE International Conference on Tools with Artificial Intelligence*, vol. 1, pp.197-204, (2008)
- [16] S.W. Ekanayake, and P.N. Pathirana, "Formations of Robotic Swarm: An Artificial Force Based Approach", *International Journal of Advanced Robotic Systems*, vol. 6(1), pp. 7-24, (2009)
- [17] A. Noack, "Modularity clustering is force-directed layout" *Physical Review E* 79, 26102, (2009)

-
- [18] C.W. Reynolds, "Flocks, Herds, and Schools:A Distributed Behavioral Model",*Computer Graphics*, **21**(4), pp. 25-34, (1987).
 - [19] G. Picard and M-P. Gleizes, "Cooperative self-organization to design robust and adaptive collectives," ICINCO 2005,pp. 236–241, (2005)
 - [20] D.Martin-Guillerez, J. Fanchon .Discrete-time simulator for wireless mobile agents.IntelNet 2010, pp.779-784, (2010)